Journal of Engineering and Sustainable Development
Vol. 30, No. 04, July 2026
https://jeasd.uomustansiriyah.edu.iq/index.php/jeasd
ISSN 2520-0917
Research Article
https://doi.org/10.31272/jeasd.4021

Demand-Response Energy Management for Renewable-Based Electric Ship Microgrids

Naveen Kumar Thotakanama[1], Nagaraja Rao Sulake[2*], Krishnan Manickavasagam[3]

[1,2] Department of Electrical Engineering, Ramaiah University of Applied Sciences, Bangalore, India
[3] Department of Electrical and Electronics Engineering Education, NITTTR, Bhopal, India

[*]Email: nagarajarao.ee.et@msruas.ac.in

Article Info

Received 12/04/2026
Revised 23/06/2026
Accepted 27/06/2026

Abstract

Electrically driven ships operate as self-contained renewable microgrids that combine power from solar and wind, along with battery energy storage, to supply propulsion and auxiliary loads. Their operation depends on the real-time coordination of distributed sources under varying environmental and load conditions. This study introduces an Artificial Neural Network-based surrogate model for the Demand-Response Energy Management System (DREMS) framework that performs real-time scheduling of renewable and dispatchable sources to meet the load requirement. This lightweight model serves as a data-driven surrogate for estimating solar and wind power outputs using meteorological data as inputs. These estimates are used by the DREMS, together with load and storage conditions, to determine optimal scheduling decisions for all power units. The approach is validated through simulations in MATLAB/Simulink using practical wind and irradiance profiles from publicly available data. The simulation results demonstrate the capability of the proposed framework to maintain supply-demand balance, coordinate renewable-energy unit commitment, and support stable operation under varying renewable-generation and load conditions. Although the study focuses on an electric-driven ship, the proposed framework can be applied to isolated renewable microgrids with similar operating conditions.

Keywords: Artificial Neural Network, Demand-Response, Electric Ship Microgrid, Renewable Energy Systems, Surrogate Model.

1. Introduction

Electrically driven ships are designed as self-sustaining power systems in which all onboard equipment depends on the internal microgrid. These vessels consist of Renewable Energy Sources (RES), power-electronic converters, and a Battery Energy Storage System (BESS) integrated into a compact structure. The absence of connected grids and the dynamic nature of operating conditions make these microgrids distinct from land-based systems. Shipboard microgrids operate under constraints that include space, weight, and reliability, making power coordination challenging when multiple subsystems compete for limited generation [1]. The integration of RES introduces variability, as changes in irradiance and wind speed directly affect power availability [2].

Control challenges are significant when dealing with power-electronic interfaced generation systems. Electric-driven ships require proper design of power converters and compensators to achieve desired voltage quality with reduced harmonic distortion [3]. A complete model of a DC shipboard microgrid that emphasizes propulsion performance depends strongly on the interactions among RES units, storage elements, and mission-dependent loads [4]. A model-predictive voltage control method for all-electric-driven ships shows that rapid disturbances in load and generation can destabilize the DC bus due to inadequate management [5]. Investigations on load-frequency control for hybrid electric-driven ships found that RES intermittency amplifies deviations during low-inertia operation [6]. Battery-electric propulsion for container ships with optimal energy dispatch is critical for achieving extended range, mission reliability, and enabling better real-time coordination [7]. An intelligent Energy-Management System (EMS) for RES-driven ships with decentralized decision-making can greatly enhance performance [8]. These studies reveal that real-time scheduling in shipboard microgrids remains challenging due to the stochastic nature of RES.

Cabrera-Tobar et al. in [9] emphasized optimization and control frameworks and their importance in addressing the stochastic nature of RES while reducing computational burden. Energy management in RES-based microgrids emphasizing uncertainty modeling and predictive capabilities is crucial for sustainable

operation under variable conditions [10]. A hierarchical deep learning approach for networked microgrids improves scheduling accuracy with substantial computational requirements [11]. Machine-Learning (ML) enhanced coordination mechanisms have also been explored for interconnected microgrids, where intelligent resource-compensation strategies improve renewable-energy utilization and operational flexibility under dynamically changing conditions [12]. Hierarchical energy-management architectures have also been developed to coordinate multiple interconnected microgrids, enabling improved energy sharing, storage utilization, and operational reliability through multi-layer supervisory control [13]. A model predictive control strategy for RES microgrids with battery systems provides superior performance through predictive regulation at the expense of higher computational complexity [14]. Deep reinforcement learning techniques have recently been applied to microgrid energy management, enabling adaptive scheduling of flexible loads and distributed energy resources under uncertain operating conditions [15]. However, most of these approaches focus on either predictive modeling or control strategies independently, with limited integration between real-time prediction and Demand-Response (DR) scheduling. In addition, their application in electric-driven ship microgrids remains limited due to computational complexity and lack of lightweight implementation.

DR reduces operational cost and emissions in RES microgrids by promoting load participation during supply shortages [16]. Distributed DR scheduling in a grid-connected microgrid enhances economic efficiency [17]. A DR-based resource-assignment method improves the balance between supply and demand [18]. Despite the benefits of DR in land-based RES-driven systems, its application in shipboard microgrids warrants further exploration. But most studies look at DR and Digital Twin (DT)-based prediction as separate components, making them less useful for coordinated real-time energy management. This shows the need for a single framework that combines lightweight prediction models with demand-adaptive scheduling for real-world shipboard operations.

Along with these developments, DT technology has emerged as a promising approach for monitoring and controlling energy systems. DT applications for smart energy systems were reviewed, with an emphasis on their role in enabling real-time decision-making [19]. DT and ML technologies for energy systems can improve forecasting, optimization, and operational reliability [20]. Recent studies have further explored AI-driven DT frameworks for renewable energy systems, in which data-driven optimization and predictive analytics support real-time operational decision-making under dynamic conditions [21]. Recent studies have also highlighted the growing importance of adaptive and intelligent operational frameworks in modern power systems, where real-time decision support and system-wide coordination contribute to improved reliability under dynamic operating conditions [22]. A lightweight DT can significantly improve closed-loop control performance in predictive power management systems [23]. Digital technologies are increasingly utilized in RES to boost efficiency and safety [24]. Many DT architectures suffer from computational complexity and are unsuitable for embedded maritime applications with limited processing resources [25]. However, many DT implementations involve complex architectures and high computational requirements, which limit their applicability in embedded shipboard systems.

Among ML techniques, Artificial Neural Networks (ANNs) are effective at handling nonlinear interactions in energy systems with reduced computational cost [26], [27]. Application of supervised learning techniques in microgrid energy management to handle stochastic solar power showed that data-driven prediction improves decision consistency [28]. Recent studies have further highlighted the growing role of deep learning-based automation techniques in power systems, where architectures such as CNNs, LSTMs, and deep neural networks support forecasting, intelligent decision-making, and enhanced operational reliability [29], [30]. ML-based forecasting and energy-management frameworks have also demonstrated improved prediction accuracy and resource-scheduling capability in renewable-energy-based microgrids through data-driven estimation of distributed-generation outputs [31]. Aloo et al. [32] developed a GA-ANFIS model for Photovoltaic (PV) – wind microgrids that accurately captured hybrid generation behavior. Foundational physical models of Permanent Magnet Synchronous Generator (PMSG) based wind energy systems presented in [33] and [34] provide a basis for generating representative datasets used to train ANN-based DTs. This makes ANN suitable for developing low-complexity surrogate models that can be implemented for real-time shipboard energy management.

Despite these advancements, significant research gaps remain for electric-driven ships. Existing shipboard control strategies rarely integrate DT-based prediction with DR scheduling, even though both techniques address complementary challenges. Many DT-based forecasting methods primarily focus on comprehensive system modeling, while lightweight, real-time implementations for shipboard applications remain an active research area. Similarly, dynamic DR strategies hardly use DT predictions to manage distributed RES optimally. As a result, the lack of a unified system that combines rapid predictions, flexible load coordination, and RES scheduling limits the operational reliability of shipboard microgrids, especially under uncertainty.

To overcome these challenges, this study proposes a lightweight ANN-based surrogate model for Demand-Response Energy Management System (DREMS) designed specifically for electric-driven ships. A compact feed-forward ANN is developed as a lightweight surrogate model to estimate instantaneous solar and wind power generation from real-time meteorological inputs. These estimates are utilized within a distributed DR control mechanism that coordinates flexible loads, multiple identical RES units, and BESS. The proposed DREMS framework is validated using practical irradiance, wind speed, and load profiles. The framework provides a systematic scheduling mechanism that integrates ANN-based renewable power estimation, DR control, renewable energy unit commitment, and battery coordination into a unified energy management structure. It also offers a computationally efficient and practically implementable solution for next-generation RES-powered electric-driven ship microgrids. The novelty of

the proposed framework lies in integrating ANN-based renewable power estimation and DR scheduling within a unified low-complexity energy management architecture for electric-driven ship microgrids. Unlike ANN-based forecasting approaches that focus primarily on prediction, MPC-based methods that require repeated online computations, fuzzy logic systems that depend on expert-defined rule sets, and conventional rule-based energy management strategies with limited adaptability, the proposed DREMS integrates lightweight ANN-based renewable power estimation with DR scheduling in a unified framework. The proposed approach is implemented using a simple architecture suitable for real-time shipboard microgrid operation.

The principal contributions of the proposed work are as follows:

- Developing a lightweight ANN-based surrogate model that can be used to estimate the outputs of RES in shipboard microgrids in real time.
- Integrating DR control with real-time energy management for better load balancing and reduced switching operations.
- Developing a scheduling framework suitable for low complexity and varying operating conditions on board.

2. Method of the Research

This section discusses shipboard microgrid configuration, RES modeling, load demand representation, and the ANN-based surrogate model development for energy management.

2.1. System Description

The electric-powered ship considered in this study functions as an autonomous microgrid with RES. As illustrated in Fig. 1, the system has Solar Power Conversion System (SPCS) units, Wind Power Conversion System (WPCS) units, a BESS, propulsion and auxiliary loads that are interconnected by a DC bus.

Maximum Power Point Tracking (MPPT)-based DC–DC boost converters connect all SPCS units to the DC bus. The small wind turbines used in the WPCS units are direct-driven Permanent Magnet Synchronous Generator (PMSG) models. These small renewable energy units can be installed on board, where weight, maintenance, and space constraints are critical.

The SPCS and WPCS units operate within the input ranges that were set during data generation for model development. When the input conditions are very low, the output power is negligibly small, and for high input conditions, the generation is dangerously high, so that the system is uncontrollable, leading to hazards. To avoid these consequences, the units beyond the operating input limits are isolated for safety and efficiency reasons.

A bidirectional converter connects the BESS to the DC bus and enables it to store surplus renewable energy and use it during deficit conditions. This reduces frequent switching of RES units, thereby improving operational reliability. A non-interruptible propulsion drive and several auxiliary subsystems make up the ship's loads. Categorizing these loads helps support DR actions.

This setup is the foundation for building the models and proposed DREMS framework.

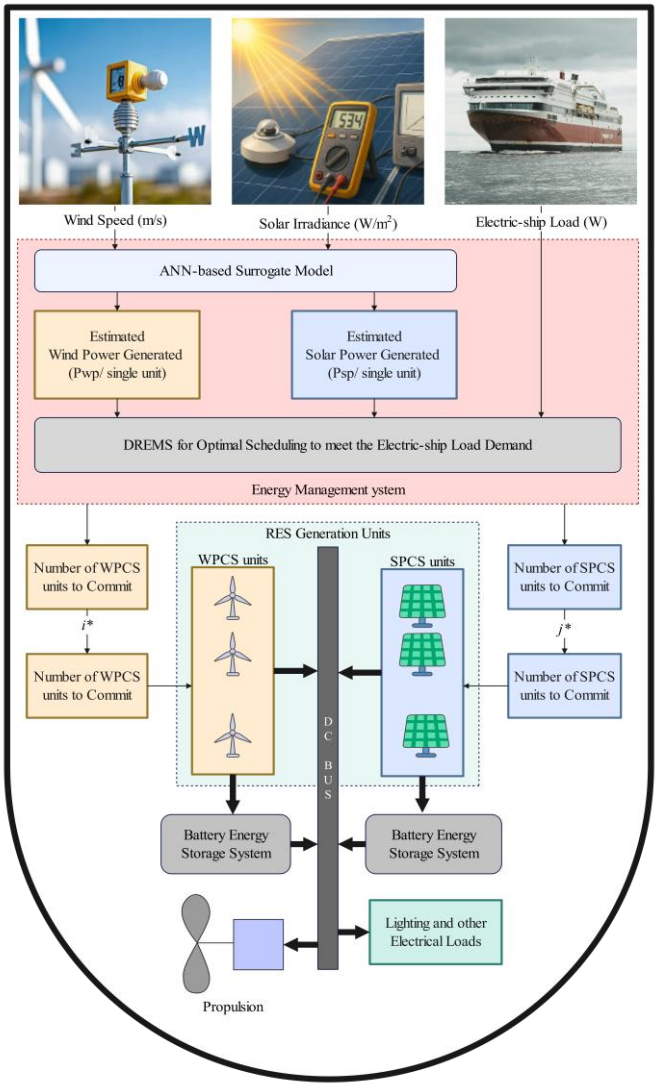

Figure 1. Overall architecture of the proposed ANN-based DREMS for a renewable-based electric-driven ship microgrid.

2.2. Renewable Energy Conversion Models

Physics-based models were developed in MATLAB/Simulink to create the SPCS and WPCS units on the shipboard microgrid. These models provide the input and output data needed to train the ANN-based surrogate model. The subsections below give a brief overview of the most important parts of each RES unit and the assumptions that were made during the simulation.

2.2.1. Solar Power Conversion System (SPCS)

The SPCS units are assumed to be identical units rated at 5 kW each. The output of each unit varies with incident irradiance and temperature over the operating range considered during data generation. The overall I-V and P-V characteristics of the PV module are shown in Fig. 2.

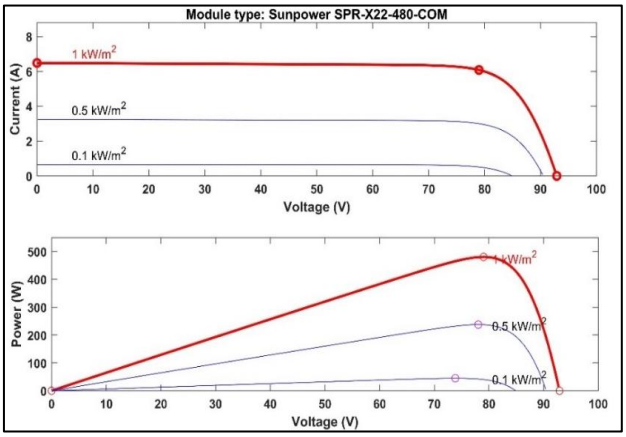

Figure 2. Current–voltage (I–V) and power–voltage (P–V) characteristics of the PV module under various irradiance levels.

A single-diode model is used to represent the PV module with a balance between modeling accuracy and computational simplicity. The terminal current is obtained from:

$$I_{pv} = I_{ph} - I_o(e^{\frac{V_{pv}+I_{pv}R_S}{nV_t}} - 1) \quad (1)$$

where I_{pv} is the module current and V_{pv} is the module voltage, I_{ph} is the photocurrent, I_0 is the diode saturation current, R_s is the series resistance, n is the diode ideality factor, and V_t is the thermal voltage. The output power P_{pv} of the module is given by:

$$P_{pv} = V_{pv}\, I_{pv} \quad (2)$$

These expressions generate the I–V and P–V performance curves used to generate the dataset for training the ANN-based surrogate model discussed in Section 3. At very low irradiance, the PV output approaches zero, and the corresponding unit is isolated in the scheduling logic. The MPPT-based boost converter adjusts the operating point to track the maximum available power during normal operating conditions.

2.2.2. Wind Power Conversion System (WPCS)

The WPCS units, each rated at 5 kW, convert the kinetic energy of wind into electrical power supplied to the DC bus through an AC–DC interface. The aerodynamic power captured by the turbine is expressed as:

$$P_{aero} = \frac{1}{2}\rho A C_p(\lambda) v^3 \quad (3)$$

where C_p is the power coefficient, ρ is the air density, A is the swept area of the turbine, and v is the wind speed.

The tip-speed ratio λ is defined as

$$\lambda = \frac{\omega_r R}{v} \quad (4)$$

with ω_r the rotor speed and R the blade radius.

The mechanical power transferred to the PMSG is converted to electrical power according to

$$P_w = \eta_g P_{\text{aero}} \quad (5)$$

where η_g is the combined generator–rectifier efficiency.

This model represents the dependence of wind power on instantaneous wind speed within the operating range relevant to shipboard installations.

For this study, the turbine operates from 3 m/s to 14 m/s. Below the cut-in and above the cut-out thresholds, output is assumed negligible. The resulting electrical power samples constitute the wind-side dataset used for training the ANN-based surrogate model described in Section 3. Fig. 3 shows the wind turbine aerodynamic characteristics and the resulting PMSG power curve.

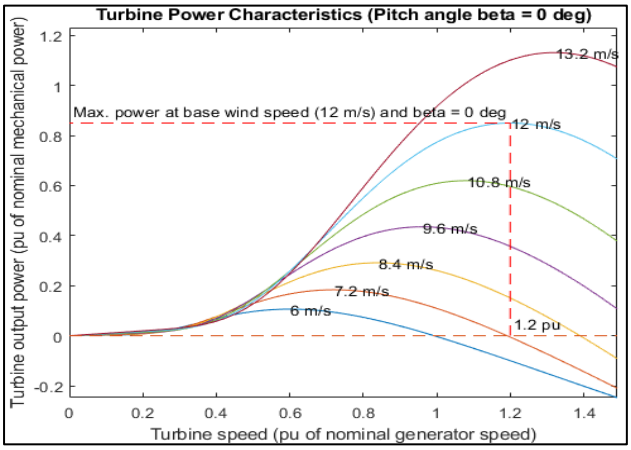

Figure 3. Wind turbine aerodynamic power characteristics for different wind speeds and the corresponding operating region.

2.3. Shipboard Load Modeling

The electric-driven ship is represented using a 24-hour load profile that captures typical variations in propulsion, navigation, auxiliary, and hotel loads. The demand ranges from low early-morning values to peak levels during propulsion-intensive periods. The load profile used in this work is shown in Fig. 4, where the horizontal axis represents time in hours and the vertical axis represents load demand in kW and serves as the baseline for all simulation scenarios discussed in Section 5.2.

3. ANN-Based Surrogate Model Development

The model developed in this work provides a fast surrogate representation that estimates the instantaneous output of RES using measured irradiance and wind speed. While Section 2 presented the physics-based PV and wind models used to generate reference data, this section describes converting these datasets into lightweight ANN-based surrogate models suitable for real-time scheduling. The developed surrogate model captures the operating behavior of RES across their valid input ranges and provides power-estimation inputs to the energy management layer.

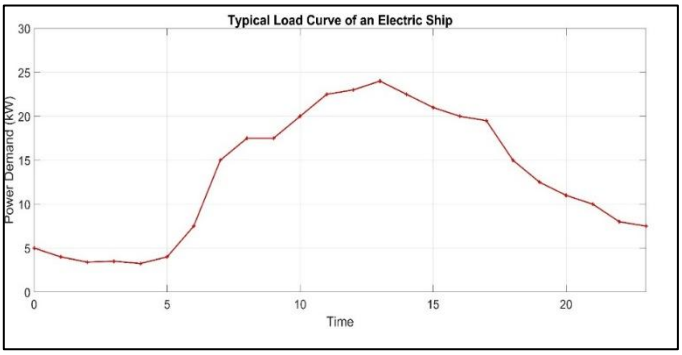

Figure 4. Typical 24-hour load profile of the electric-driven ship used in the simulation.

3.1. Data Preparation for the Surrogate Model

The surrogate models require representative datasets linking meteorological inputs to the electrical power output of RES. Using the physics-based models described in Section 2, the WPCS and SPCS were simulated in MATLAB/Simulink across their full operating ranges. A stepwise wind speed profile was applied to the WPCS model, and a similar irradiance sweep was used for the SPCS model. The corresponding power outputs were recorded to form clean, monotonic datasets suitable for ANN training.

Zero-generation samples beyond the operating ranges of wind speed or irradiance were removed. All variables were normalized to [0,1] using min–max scaling, and the resulting dataset was shuffled and split into training (80%), validation (10%), and test subsets (10%). Data samples were randomly divided using MATLAB's default data-partitioning approach (dividerand). The validation subset was used to monitor generalization performance during training and to reduce the possibility of overfitting. This ensures that the ANN model is trained on representative conditions and evaluated on unseen samples.

Fig. 5 presents the full dataset used for surrogate model development, including the wind speed versus WPCS power curve and the irradiance versus SPCS power curve.

3.2. ANN Model Development

The surrogate model is implemented using two lightweight feed-forward ANNs, one for the SPCS and one for the WPCS. Each ANN receives a single meteorological input, irradiance for the SPCS and wind speed for the WPCS, and outputs the corresponding instantaneous electrical power of a renewable energy unit.

Both models employ a single hidden layer with seven neurons, constructed in MATLAB using a feedforwardnet (7). The hidden layer utilizes the default MATLAB sigmoid activation function, while the output layer works with a linear activation function suitable for continuous power estimation. This structure was chosen to maintain a low computational burden while preserving the nonlinear mapping between input and output. The ANN architecture was intentionally kept compact to maintain model simplicity and computational efficiency. A single hidden layer with seven neurons provided satisfactory regression performance for the available training data and was therefore adopted for surrogate model development.

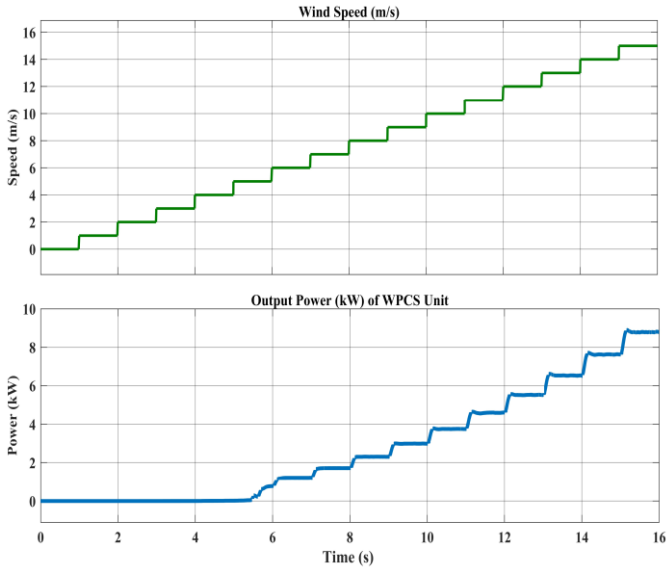

(a) Wind speed and corresponding WPCS output power.

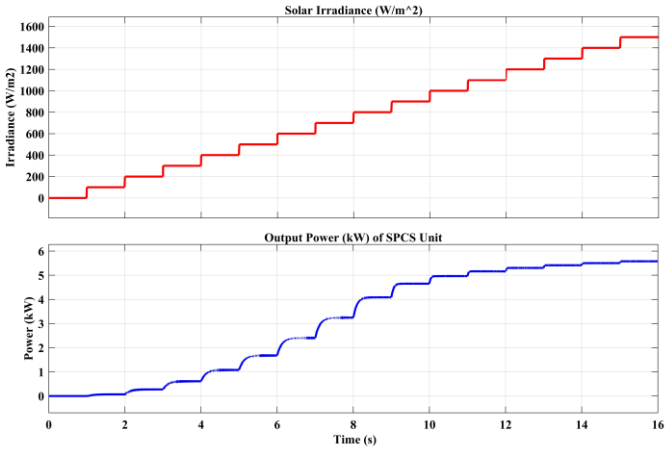

(b) Solar irradiance and corresponding SPCS output power.

Figure 5. Input–output datasets used to train the ANN surrogate models.

Hyperparameter optimization was not considered in this study because the objective was to develop a lightweight surrogate model for energy management applications rather than investigate ANN architecture optimization. The ANN formulation for each model can be written as:

$$\hat{P}(k) = f(W_2\,\phi(W_1\,u(k) + b_1) + b_2) \quad (6)$$

where $u(k)$ is the normalized input (irradiance or wind speed), $P(k)$ is the estimated power, W_1 and W_2 are weight matrices, b_1 and b_2 are bias vectors, $\phi(\cdot)$ is the hidden-layer activation function, and $f(\cdot)$ is the linear output activation function.

Both ANNs were trained using backpropagation for up to 2000 epochs. The networks were trained using the Levenberg-Marquardt backpropagation algorithm (trainlm) with mean squared error (MSE) as the performance function. Default

MATLAB training parameters were used throughout the training process, and no manual adjustment of the learning rate was performed. The loss function minimized during training is the mean-squared error (MSE):

$$J = \frac{1}{N}\sum_{k=1}^{N}(P(k) - \hat{P}(k))^2 \quad (7)$$

where $P(k)$ represents the target power samples that were extracted from the physics-based models in Section 2.

During training, the MSE decreased progressively and reached convergence within the specified training epochs. The validation dataset was used to monitor generalization performance and prevent excessive overfitting. The regression results presented in Section 3.3 confirm that the trained networks achieved satisfactory convergence and estimation accuracy.

This compact ANN architecture lets the surrogate models run with low computational delay, which makes them good for real-time scheduling in the DREMS framework.

3.3. Training and Validation of ANN Model

The datasets described in Section 3.1 were used to train the ANN-based surrogate models for SPCS and WPCS. To assess the learning performance, MATLAB regression plots were created for both networks.

Fig. 6 (a) displays the regression outcomes for the SPCS model, indicating that the estimated values closely align with the target samples across all subsets. The overall correlation coefficient (R) is about 0.98, which implies the ANN accurately shows the relation between the irradiance and power of one SPCS unit.

In a similar way, Fig. 6 (b) shows the regression results for the WPCS model. The estimated output is very close to the target power for all wind speeds, with an overall correlation coefficient (R) value of about 0.99. This indicates that the ANN can accurately model the nonlinear aerodynamic and electromechanical behavior of the PMSG-based WPCS.

The strong correlation in both cases shows that the compact ANN structure is good for real-time use, providing the scheduling logic with power estimates required for scheduling decisions. The regression results demonstrate that the ANN provides accurate power estimation across the operating range of the renewable energy units.

3.4. Justification for the Lightweight ANN-based Surrogate Model

The ANN model acts as a lightweight surrogate model; it uses real-time measurements of irradiance and wind speed to mimic the behavior of the SPCS and WPCS units in terms of instantaneous power. The validated physics-based models in Section 2 provide the data required for the network training. This lets it learn how the electrical output changes in response to different environmental inputs across the operating range of the onboard units.

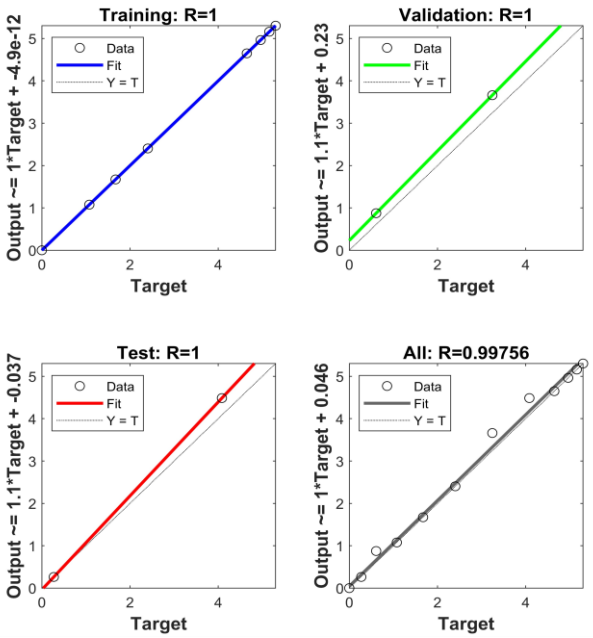

(a) SPCS regression plot.

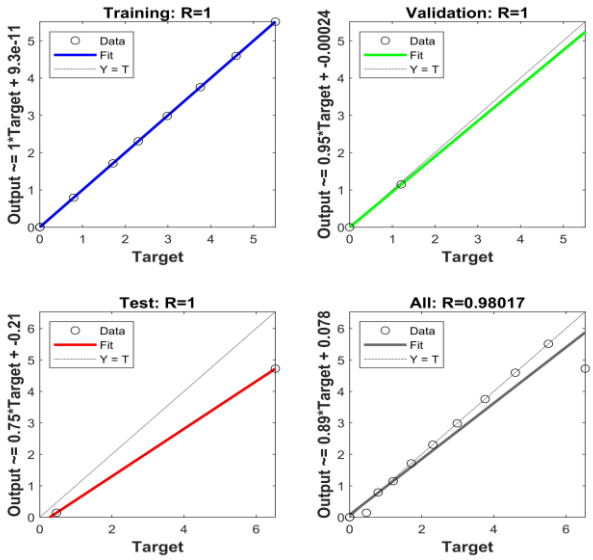

(b) WPCS regression plot.

Figure 6. Regression performance of the ANN-based surrogate model (a) SPCS, (b) WPCS, showing the training, validation, testing, and overall correlation between target and estimated power outputs.

Compact architecture, comprising a single hidden-layer ANN with seven neurons, is suitable for implementation on embedded shipboard controllers. Unlike stand-alone regression or forecasting models, the ANN works directly within the energy management loop, giving continuous power estimates that help with generator scheduling and DR decisions. These real-time operating capabilities make it a lightweight and effective surrogate model for estimating renewable power output in electric-driven ships. Alternative ML techniques such as ANFIS, Random Forest, LSTM, and deep neural networks

may also be applied for renewable power estimation. However, the objective of this work is to develop a computationally efficient surrogate model for integration with the proposed DREMS framework rather than conduct a comparative evaluation of ML algorithms. A comprehensive comparison of alternative ML approaches is considered for future investigation.

The ANN-based surrogate model serves as a virtual representation of the renewable power units by reproducing their input-output behavior using environmental measurements. In this sense, the surrogate model performs the modeling function commonly associated with the virtual layer of a DT. However, the proposed framework focuses on lightweight real-time power estimation and scheduling rather than implementing a complete cyber-physical DT architecture.

4. Demand-Response Energy Management System (DREMS)

As explained in Section 3, the DREMS framework uses real-time estimates from the ANN-based surrogate model to control RES units, BESS, and loads on board the ship. At each control step, the controller gets the estimated PV and wind power, the measured load demand, and the battery state of charge (SOC). These inputs are used to determine load balancing, the number of RES units to commit, and the charge and discharge control of the battery. The main goal is to meet the ship load demand while cutting down on unnecessary switching between SPCS and WPCS units.

4.1. Load Classification for Demand-Response Scheduling

For DR scheduling, the total demand on the ship is divided into critical and flexible loads. Propulsion drives, navigation, communication systems, and other important auxiliary parts that need to be constantly supplied are all examples of critical loads. HVAC systems, service utilities, and non-essential auxiliaries are all examples of flexible loads. This means that flexible load operation can be temporarily deferred or rescheduled without compromising the ship's safety.

This analysis considers the variations in demand that follow the same 24-hour load profile as in Section 2.3. This profile represents the typical operating pattern of an electric-driven ship that usually works and is the basis for making DR decisions in the suggested control strategy.

4.2. Demand-Response Control Strategy

The DR mechanism alters the operation of flexible shipboard loads depending on variations in renewable energy generation, battery SOC, and total demand. The goal is to maintain the supply-demand balance while cutting down on unnecessary switching of RES units. At each control step, the controller checks the estimated renewable power from the ANN-based surrogate model, the measured ship load, and the battery SOC.

The controller determines the extent to which the load needs to be adjusted based on these inputs. The DR mechanism modifies only the flexible-load component of the ship demand, while critical loads remain continuously supplied. Depending on the severity of the power deficit, different levels of flexible-load curtailment are applied. The resulting adjusted demand is subsequently represented mathematically in Section 4.3.1 and used for renewable-unit scheduling and battery-management decisions. All loads work normally if there is sufficient renewable power and adequate SOC. When a deficit is detected, a tiered DR action is applied:

- Level 1 (Mild): Temporary deferral of low-priority auxiliary loads.
- Level 2 (Moderate): Partial curtailment of HVAC and other flexible systems within predefined reduction limits.
- Level 3 (Severe): Only critical loads are supplied when both renewable power availability and SOC fall below acceptable thresholds.

All DR actions are applied for short durations and are re-evaluated at each control interval to avoid prolonged suppression of flexible loads. The resulting adjusted load is then used by the generator scheduling and battery management modules described in Sections 4.3 and 4.4.

4.3. Renewable Energy Unit Scheduling Strategy

In the proposed shipboard microgrid, all SPCS units are identical, and all WPCS units are identical. The ANN-based surrogate model provides the estimated power output of a single SPCS and a single WPCS unit under the current irradiance and wind speed. Denoting these single-unit outputs by $\hat{P}_{sp}$ and $\hat{P}_{wp}$, the total renewable power available for any combination of committed units(i, j) is

$$P_{\text{ren}}(i.j) = i\,\hat{P}_{sp} + j\,\hat{P}_{wp} \tag{8}$$

Where $i \in \{0,1,\dots,N_{sp}\}$ and $j \in \{0,1,\dots,N_{wp}\}$ represent the number of active SPCS and WPCS units, respectively. N_{sp} and N_{wp} are the maximum number of SPCS and WPCS units available for power generation at that instant, respectively.

4.3.1 Effective Demand After DR Adjustment

The load adjusted by the DR logic is expressed as

$$P_{\text{req}} = P_{\text{crit}} + P_{\text{flex,adj}} \tag{9}$$

where P_{crit} is the critical load and $P_{\text{flex, adj}}$ is the flexible-load demand remaining after the application of the selected DR level. Thus, the effective demand consists of the complete critical-load demand and the adjusted flexible-load component resulting from the DR strategy described in Section 4.2. The mismatch between supply and demand for any unit combination is

$$\Delta P(i,j) = P_{\text{req}} - P_{\text{ren}}(i,j) \tag{10}$$

where $\Delta P(i,j)$ denotes the power mismatch corresponding to the commitment of i SPCS units and j WPCS units. A positive value indicates that the effective demand exceeds the renewable power supplied by the committed units, whereas a negative value indicates surplus renewable generation. The mismatch is evaluated using only the committed renewable-energy units

during the scheduling stage. Any remaining surplus or deficit power is subsequently handled by the BESS management strategy described in Section 4.4.

4.3.2. RES unit commitment

For all feasible combinations (i, j), the scheduling objective is to minimize the absolute mismatch:

$$(i^*, j^*) = \arg \min_{(i,j)} | \Delta P(i,j) | \quad (11)$$

subject to operational limits:

$$0 \le i \le N_{sp};\ 0 \le j \le N_{wp};\ SOC_{\min} \le SOC \le SOC_{\max};\quad (12)$$

Because the total number of SPCS and WPCS units is considered to be five each in this study, all combinations can be evaluated in real time without requiring complex optimization algorithms. For the considered configuration, the total number of feasible unit-commitment combinations remains limited, resulting in a low computational burden that is suitable for real-time shipboard implementation. However, for larger renewable power systems with a significantly higher number of generation units, the number of feasible combinations may increase substantially. In such cases, hierarchical scheduling, optimization-based approaches, or metaheuristic techniques may be employed to reduce computational complexity while maintaining scheduling effectiveness. The scheduling algorithm evaluates all feasible unit combinations and selects the combination that yields the minimum absolute power mismatch defined in (11). Once the optimal (i^*, j^*) is obtained, the corresponding units are switched ON, and the remainder remain OFF. The remaining mismatch after committing the RES units is then handled by the BESS logic in Section 4.4. The scheduling strategy is evaluated over a 24-hour operating horizon, and the unit commitment decision is updated at each control interval using the estimated renewable power, load demand, and battery SOC.

4.4. Battery Energy Storage System Management

BESS provides fast charge–discharge support after the DR action and the RES-unit commitment from Sections 4.2 and 4.3. Using the effective demand expressed in (9) and the optimal unit combination (i^*, j^*) obtained from the scheduling block, the ANN-based surrogate model provides the estimated renewable power as

$$P_{\text{RE}} = i^* \hat{P}_{sp} + j^* \hat{P}_{wp} \quad (13)$$

The battery setpoint is then computed from the mismatch between P_{RE} and P_{req}, subject to SOC limits.

(a) Charging Mode

When renewable power generation exceeds the effective demand,

$$P_{\text{RE}} > P_{\text{req}};$$

The surplus power is utilized to charge the battery:

$$P_{\text{ch}} = \min (P_{\text{RE}} - P_{\text{req}},\ P_{\text{ch,max}}) \quad (14)$$

subject to

$$SOC < SOC_{\max} \quad (15)$$

If the maximum SOC is reached, the surplus is curtailed.

(b) Discharging Mode

When renewable power is insufficient to meet demand,

$$P_{\text{RE}} < P_{\text{req}};$$

the battery supplies power through discharging:

$$P_{\text{dis}} = \min (P_{\text{req}} - P_{\text{RE}},\ P_{\text{dis,max}}) \quad (16)$$

subject to

$$SOC > SOC_{\min} \quad (17)$$

If the SOC falls to its minimum threshold, the remaining mismatch is passed back to the scheduling and DR blocks for further action.

(c) SOC Update

SOC evolves according to

$$SOC(k+1) = SOC(k) + \frac{\eta_{\text{ch}} P_{\text{ch}} - \frac{P_{\text{dis}}}{\eta_{\text{dis}}}}{E_{\text{rated}}}\ \Delta t \quad (18)$$

where η_{ch}, η_{dis} are the converter efficiencies, E_{rated} is the battery energy capacity, and Δt is the control interval.

The battery-management strategy adopted in this work primarily focuses on maintaining supply-demand balance and preserving the battery SOC within predefined operating limits. Battery degradation mechanisms such as capacity fade, cycle aging, internal resistance growth, and temperature-dependent performance variations are not explicitly modeled in the present framework. Nevertheless, maintaining the battery SOC within prescribed operating limits helps reduce excessive charging and discharging stress, thereby supporting improved battery utilization and operational reliability. In practical shipboard applications, more advanced battery management systems may incorporate battery state-of-health estimation, degradation-aware scheduling, and optimized charging/discharging strategies to enhance battery lifetime and overall system performance. Such considerations can further improve the long-term operational effectiveness of renewable-energy-based shipboard microgrids.

4.5. Integrated ANN-based Scheduling Framework

The ANN-based DREMS controller functions as a closed-loop system, integrating surrogate model-based estimation, DR adjustment, RES-unit scheduling, and battery management. The surrogate model provides the estimated SPCS and WPCS outputs during each control iteration. These are then compared to the updated load demand, which is based on the DR rules in Section 4.2. Using these values, the scheduling algorithm finds the best combination of RES units (i^*, j^*) as explained in Section 4.3. After that, the battery either absorbs surplus power or supplies deficient power, as long as it stays within its SOC limits, as stated in Section 4.4. The overall energy management workflow integrating DR, scheduling, and battery control is illustrated in Fig. 7.

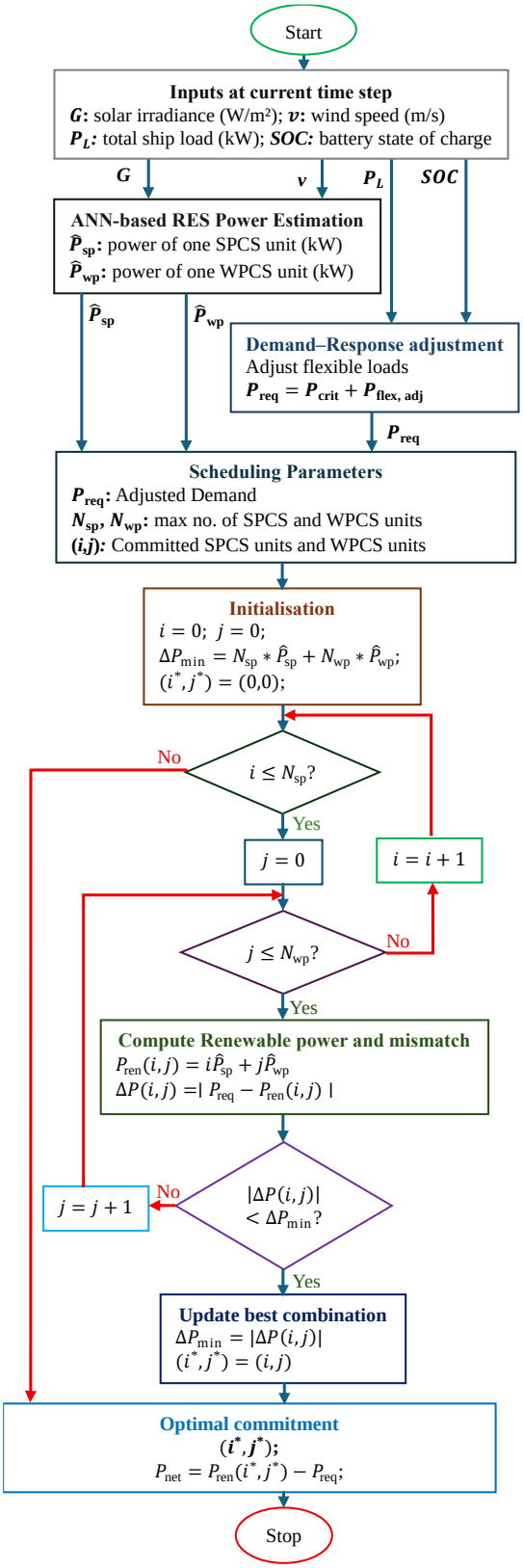

Figure 7. Flowchart of the proposed ANN-based DREMS for optimal unit commitment and power balance.

If RES power and allowable BESS support are insufficient, the DR block further reduces flexible loads to ensure an uninterrupted supply to critical loads. This sequence enables fast adjustment to changes in irradiance, wind speed, and load variations, while the ANN-based surrogate model ensures low computational burden suitable for onboard implementation.

5. Simulation Setup

This section describes the simulation environment, system parameters, test scenarios, and evaluation metrics used to evaluate the proposed ANN-based DREMS framework. All simulations were carried out in MATLAB/Simulink, combining the RES models of Section 2, the ANN-based surrogate model of Section 3, and the scheduling rules of Section 4.

5.1. System Parameters

The main parameters used in the MATLAB/Simulink simulations of the proposed ANN-based DREMS framework for the shipboard renewable microgrid are summarized in Table 1.

Table 1. System parameters used for simulation studies.

Parameter	Value
Number of SPCS units N_{sp}	5
Number of WPCS units N_{wp}	5
Rated power of each SPCS unit	5 kW
Rated power of each WPCS unit	5 kW
Battery rated energy capacity E_{rated}	100 kWh
Maximum charge power $P_{ch,\,max}$	25 kW
Maximum discharge power $P_{dis,\,max}$	25 kW
Battery charge efficiency η_{ch}	95%
Battery discharge efficiency η_{dis}	95%
SOC limits (SOC_{min}, SOC_{max})	20%, 90%
DC bus voltage	400 V
Peak ship load	25–30 kW*
Irradiance range for surrogate model	0–1200 W/m²
Wind speed range for surrogate model	0–15 m/s
Wind-turbine cut-in/cut-out speeds	3 m/s and 14 m/s

*Total ship load including critical and flexible loads.

5.2. Test Scenarios

The ANN-based DREMS framework was evaluated under four representative 24-hour operating scenarios. All scenarios use the same ship-load profile described in Section 2.3 and the parameters presented in Table 1. The meteorological inputs (irradiance and wind speed) were varied to reflect typical conditions encountered in renewable energy-based marine environments.

Scenario 1 – Normal operating day

Moderate variations in irradiance and wind speed without prolonged deficits or surges. This scenario serves as the baseline for evaluating ANN-based power estimation and DREMS scheduling under nominal conditions.

Scenario 2 – Deficient RES

In this scenario, low irradiance and light winds occur, requiring limitation of flexible loads and discharge of stored battery energy to maintain the supply-demand balance within SOC limitations.

Scenario 3 – High Renewable Energy Availability

Solar and wind power generation are abundant, and the surplus power is stored in BESS. This requires efficient utilization of renewable energy, preventing excessive curtailment and switching off RES units.

Scenario 4 – Sudden surge in load

A typical day involves a surge in propulsion demand that necessitates assessing the effectiveness of the BESS in handling transient conditions as well as the DREMS response to sudden load changes.

5.3. Evaluation Metrics

Qualitative evaluation criteria related to estimation accuracy, scheduling behavior, and overall operational stability are used to evaluate the effectiveness of the proposed ANN-based DREMS. Regression graphs used to assess the ANN-based surrogate model show a strong correlation between target and estimated RES power values for both SPCS and WPCS units. This confirms that accurate power estimates are produced by the surrogate models to enable real-time scheduling. By evaluating the committed SPCS and WPCS combinations utilized to satisfy the effective load demand during DR variations, the generator-scheduling process is examined. Since excessive switching is undesirable for shipboard systems, the unit commitment behavior and the switching activity of RES units are also examined.

The SOC progression for each test scenario is used to evaluate the BESS operational performance. A steady SOC path within acceptable bounds shows that RES supply, DR, and BESS are working in coordination. The amount of flexible-load curtailment is used to demonstrate the operation of the DR mechanism during the periods of insufficient renewable power availability. Critical loads are always preserved through the appropriate implementation of DR actions, whereby the controller manages the supply-demand balance under stochastic operating conditions.

The combination of these metrics and the time-domain results discussed in Section 6 provides a consistent and practical evaluation of the proposed strategy, considering the constraints of the available simulation data.

6. Results and Discussion

The operational performance of the proposed ANN-based DREMS framework is assessed in this section using the 24-hour simulation configurations outlined in Section 5. It is organized as follows: (i) Surrogate model input/output behavior; (ii) generator-unit commitment; and (iii) power-balance assessment utilizing load demand and available renewable power.

6.1. ANN Model Estimation Accuracy

The regression analyses shown in Fig. 6(a)–(b) of Section 3.3 have already established the estimation accuracy of the ANN-based surrogate models. The obtained regression results indicate a strong correlation between the target and estimated power outputs for both SPCS and WPCS models, confirming their suitability for real-time scheduling applications. Additional quantitative performance metrics are presented in Table 2 to further assess model accuracy.

In the simulation environment, for all irradiance and wind speed inputs used in the 24-hour test scenarios, the ANN outputs remained consistent with the physics-based power curves. Within the trained operating ranges, no abnormal deviations or saturation effects were noted. When assessing generator commitments and BESS decisions, the DREMS controller can rely on the model estimates.

The input profiles employed in this investigation are displayed in Fig. 8 (a), showing the variations in wind speed and solar irradiance given as input to the ANN model in a day. Fig. 8(b) shows the model-generated RES power outputs of one SPCS and one WPCS unit with these inputs. The response of the ANN-based surrogate model to variations in the weather data is evident from these data.

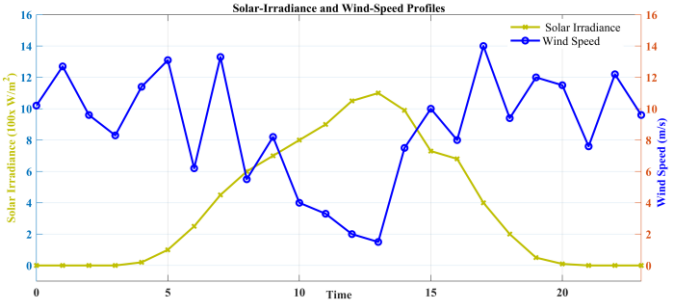

(a) Solar irradiance and wind speed curves over 24 hours.

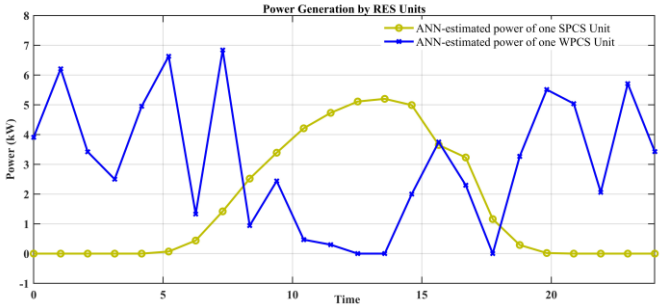

(b) ANN-estimated power outputs of one SPCS unit and one WPCS unit corresponding to inputs.

Figure 8. Input profiles and corresponding ANN-estimated power outputs of RES units.

The results presented in Fig.8 further demonstrate the capability of the ANN-based surrogate models to track variation in irradiance and wind speed while producing consistent renewable power estimates. To provide a more comprehensive assessment of model accuracy in addition to the regression coefficients presented in Section 3.3, additional statistical error metrics, namely Mean Absolute Error (MAE), Root Mean Square Error (RMSE), and Mean Absolute Percentage Error (MAPE), were evaluated and summarized in Table 2.

Table 2. Quantitative performance metrics of ANN-based surrogate models.

ANN model	R	MAE	RMSE	MAPE (%)
SPCS	0.98	0.0728	0.1645	6.30
WPCS	0.99	0.1461	0.4747	9.26

As shown in Table 2, both ANN-based surrogate models exhibit low estimation errors. The obtained MAPE values are below 10%, indicating satisfactory agreement between the ANN-estimated outputs and the reference values generated from the physics-based renewable SPCS and WPCS models. These results further confirm the suitability of the developed ANN models for renewable power estimation within the proposed DREMS framework.

6.2. DREMS Scheduling Framework

The DREMS controller was evaluated using the 24-hour irradiance and wind speed inputs. During the operating intervals, the DREMS controller scheduled the optimal number of SPCS and WPCS units to meet the effective load demand. This results in a limited number of unit commitment transitions during the scheduling horizon. The resulting unit commitment profile is presented in Fig. 9, in which the number of units turned ON is plotted over the 24-hour cycle. During periods of low renewable power generation, additional units were committed, and stored energy in the BESS was also utilized when required while maintaining SOC limits.

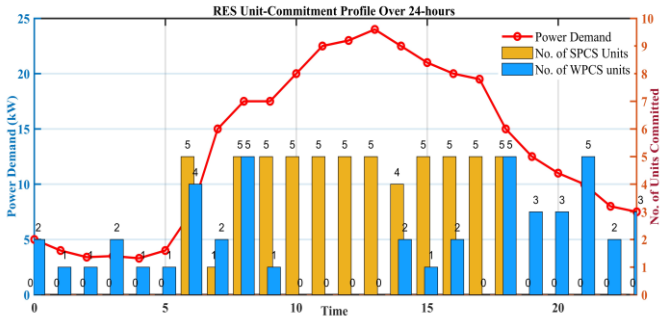

Figure 9. Number of committed SPCS and WPCS units over the 24-hour simulation period.

6.3 Operational Performance Using Hourly Data

Table 3 summarizes the hourly operational performance of the proposed ANN-based DREMS. It shows variations in solar irradiance, wind speed, RES power generation, load demand, RES unit commitment, and the related surplus or deficit over a 24-hour period. Fig. 10 shows the combined impact of load demand and available renewable power.

During the daytime, especially from 08:00 to 15:00 hours, the system functions at surplus conditions, wherein the combined solar and wind power generation surpasses the vessel's electrical demand. For instance, from 12:00 to 14:00, increased solar irradiation in combination with normal wind speeds produces surplus power of around 1.4 kW to 2.6 kW. During these periods, the DREMS controller directs surplus power to battery charging while maintaining the SOC within the specified upper limit. Upon reaching its permissible charging limit, any excess power is curtailed to prevent overcharging.

During periods of insufficient renewable power availability, notably at 17:00, a substantial power deficit of approximately 13.7kW is observed. This occurs due to reduced wind speed and solar irradiance, combined with a comparatively increased load demand. Under this scenario, the controller commits the available RES units to their highest permissible configuration and initiates battery discharge. When RES generation and BESS support are inadequate, the DR mechanism is initiated to reduce flexible loads, while ensuring a continuous supply to essential loads. A minor deficit observed at 20:00 hours (–0.92 kW) is entirely balanced by BESS discharge, avoiding the initiation of DR activities.

Although the proposed DREMS framework demonstrates satisfactory performance under the considered simulation scenarios, the ANN surrogate models were trained using datasets generated from validated physics-based SPCS and WPCS models implemented in MATLAB/Simulink. The absence of experimental or real shipboard operational data represents a limitation of the present study. Future work will focus on validating the proposed framework using measured renewable-power and load-demand data obtained from practical shipboard or isolated microgrid installations.

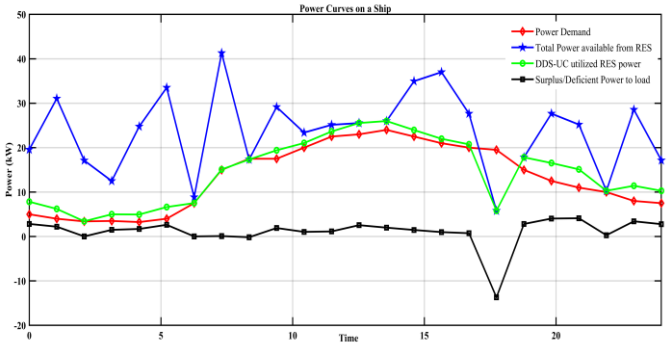

Figure 10. 24-hour power-management profile showing load demand, available renewable power, DREMS-utilized renewable power, and the resulting surplus/deficit power balance.

The overall power balance profile shown in Fig. 10 illustrates that surplus intervals are directly associated with BESS charging phases, whereas deficit intervals indicate BESS discharging or DR activation. During the entire 24-hour operational cycle, the DREMS controller maintains a stable operation with continuous supply to all essential loads while keeping the battery within safe operational limits.

The results show that the proposed ANN-based DREMS coordinates RES availability, battery constraints, and shipboard load prioritization under varying environmental and demand conditions.

6.4. Comparative Benchmarking of Energy Management Strategies

A qualitative comparison between the proposed DREMS technique and a conventional rule-based energy management

strategy commonly used in small RES microgrids was conducted. Rule-based controllers generally rely on static threshold logic (e.g., irradiance or wind speed thresholds) to engage or disengage RES units, offering limited flexibility in response to rapid fluctuations in load and source availability. These systems do not integrate forecasting, resulting in reactive responses that may increase switching activity and dependence on storage or auxiliary power sources under certain operating conditions.

The qualitative performance trends observed in this study agree with established behavior of rule-based control strategies reported in the literature [35]. To compare the two methods in terms of forecasting ability, supply-demand matching, switching behavior, auxiliary-power dependence, and adaptability under dynamic marine conditions, a set of functional indicators was established. Due to the absence of a directly simulated rule-based benchmark in this study, the comparison is presented qualitatively, based on established operational characteristics reported in the literature.

Table 3. Hourly renewable power availability, load demand, unit commitment, and surplus/deficit power.

Time	Solar Irradiance (W/m^2)	P_{sp} (kW)	Wind Speed (m/s)	P_{wp} (kW)	Electric Load (kW)	SPCS Units	WPCS Units	Committed RES power (kW)	Pexcess (kW)
00:00	0	0.000	10.2	3.913	5.0	0	2	7.826	2.83
01:00	0	0.000	12.7	6.211	4.0	0	1	6.211	2.21
02:00	0	0.000	9.6	3.423	3.4	0	1	3.423	0.02
03:00	0	0.000	8.3	2.499	3.5	0	2	4.998	1.50
04:00	20	0.003	11.4	4.948	3.3	0	1	4.948	1.70
05:00	100	0.070	13.1	6.632	4.0	0	1	6.632	2.63
06:00	250	0.443	6.2	1.327	7.5	5	4	7.522	0.02
07:00	450	1.422	13.3	6.838	15.0	1	2	15.098	0.10
08:00	600	5.523	5.5	0.944	17.5	3	1	17.513	0.01
09:00	700	3.394	8.2	2.436	17.5	5	1	19.406	1.91
10:00	800	4.208	4	0.470	20.0	5	0	21.040	1.04
11:00	900	4.728	3.3	0.299	22.5	5	0	23.640	1.14
12:00	1050	5.109	2	0.000	23.0	5	0	25.545	2.55
13:00	1100	5.198	1.5	0.000	24.0	5	0	25.990	1.99
14:00	990	4.992	7.5	1.999	22.5	4	2	23.966	1.47
15:00	730	3.648	10	3.753	21.0	5	1	21.993	0.99
16:00	680	3.227	8	2.304	20.0	5	2	20.743	0.74
17:00	400	1.161	14	0.000	19.5	5	0	5.805	-13.70
18:00	200	0.292	9.4	3.273	15.0	5	5	17.825	2.82
19:00	50	0.019	12	5.514	12.5	0	3	16.542	4.04
20:00	10	0.001	11.5	5.038	11.0	0	2	10.076	-0.92
21:00	0	0.000	7.6	2.058	10.0	0	5	10.290	0.29
22:00	0	0.000	12.2	5.709	8.0	0	2	11.418	3.42
23:00	0	0.000	9.6	3.428	7.5	0	3	10.284	2.78

The rule-based EMS reacts to real-time observations, whereas the proposed DREMS incorporates ANN-based renewable-power estimation to support scheduling decisions under varying load and resource conditions. As a result, rapid changes in operating conditions can lead to large power imbalances. The proposed DREMS, in comparison, employs surrogate-model-based estimates to anticipate renewable power availability and commits only the required SPCS and WPCS units. This reduces frequent switching actions and improves overall utilization of RES. The DREMS also exhibits improved load adaptability by integrating DR actions, whereas rule-based logic typically curtails flexible loads only after significant deficits occur. Overall, the proposed strategy demonstrates stable operation and coordinated management of renewable-power estimation, DR actions, and RES-unit scheduling under the investigated operating conditions.

Table 4 presents a qualitative benchmarking of different EMS approaches based on commonly reported characteristics in the literature [14]-[16], [18], [34] and their suitability for renewable microgrid applications. Fig. 11 visualizes the corresponding normalized qualitative scores (scale: 1-5) for rule-based EMS and proposed DREMS.

As shown in Table 4, advanced EMS approaches such as fuzzy-logic, MPC-based, and optimization-based methods generally provide improved adaptability compared with conventional rule-based control. However, these approaches often rely on expert-defined rules, repeated online computations, or optimization procedures. The proposed ANN-DREMS combines renewable power estimation, DR scheduling, and RES-unit commitment within a computationally simple framework suitable for real-time shipboard implementation.

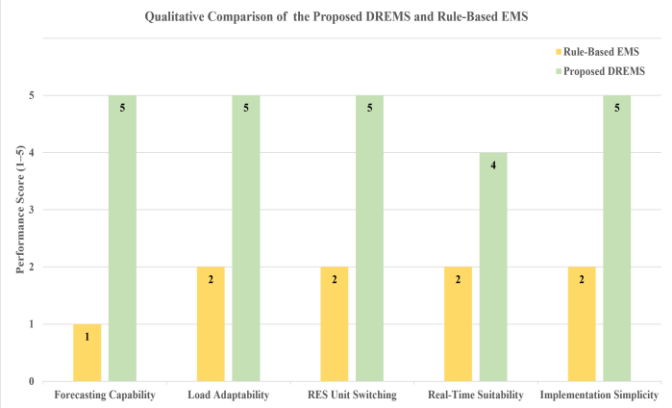

Figure 11. Qualitative Performance Comparison of the proposed DREMS and a conventional Rule-Based EMS

Note: The scores shown in Fig. 11 are qualitative assessments derived from the comparative characteristics summarized in Table 4 and do not represent results obtained from direct numerical simulation of rule-based EMS.

Table 4. Comparative benchmarking of energy management strategies.

Feature	Rule-based EMS	Fuzzy Logic EMS	MPC-based EMS	Optimization-based EMS	Proposed ANN-DREMS
Forecasting Capability	Not available	Not available	Possible	Possible	ANN-based estimation
DR Integration	Limited	Moderate	Good	Good	Integrated
Load Adaptability	Reactive	Moderate	High	High	Real-time response
Computational Complexity	Low	Moderate	High	High	Low
RES Unit Switching	Excessive	Moderate	Reduced	Reduced	Minimum switching
Renewable Power Estimation	No	No	Possible	Possible	Yes
Real-Time Suitability	High	Moderate	Moderate	Limited	High
Shipboard Implementation Simplicity	High	Moderate	Low	Low	High

6.5. Robustness and Practical Considerations

The robustness of the proposed DREMS was assessed under varying renewable power generation and load conditions using practical irradiance, wind speed, and shipboard load profiles. The ANN-based surrogate models provided accurate estimates of renewable power across different operating conditions, enabling the scheduling framework to adapt to fluctuations in resource availability and demand. The DR mechanism further enhanced operational flexibility by adjusting the committed RES units according to the prevailing power-balance requirements.

It should be noted that sensor noise, battery degradation effects, and converter losses were not explicitly modeled in the present study. The objective of this work was to establish and validate the proposed ANN-assisted DREMS framework under representative operating conditions using validated renewable power conversion models. Future work will focus on incorporating measurement uncertainty, battery aging characteristics, converter non-idealities, and hardware-in-the-loop or real-time validation to further evaluate the robustness of the proposed approach under practical shipboard operating environments.

7. Conclusion

This work presented an ANN-based DREMS framework for an electric-driven ship operating as a standalone renewable microgrid. The proposed approach integrates lightweight ANN-based surrogate models for SPCS and WPCS with a sequential scheduling logic that coordinates RES commitment, BESS operation, and flexible-load adjustments. The surrogate models successfully captured the nonlinear characteristics of the RES units, enabling fast estimation of available power without relying on the full physics-based subsystem models.

Simulation studies demonstrated that the proposed DREMS maintained continuity of supply to critical ship loads while adapting to variations in irradiance, wind speed, and propulsion-driven load changes. The controller committed the required SPCS and WPCS units while maintaining battery SOC within the defined operating limits and adapting to variations in renewable generation and load demand. To preserve stable ship operations, DR activities were restricted to flexible loads and executed during instances of insufficient power generation.

The results demonstrate the capability of the proposed DREMS to integrate ANN-based renewable-power estimation, DR coordination, RES-unit scheduling, and battery management within a unified energy-management framework. The developed approach supports load-supply balancing, renewable-energy utilization, and operational flexibility for electric-driven ship microgrids.

Future work may concentrate on refining surrogate models to incorporate long-term forecasting, integrating the DREMS with optimization-driven scheduling techniques, and evaluating the framework on hardware-in-the-loop and real-time platforms conducive to onboard implementation. Further investigation of cyber-physical implementation aspects, including communication delays, measurement uncertainties, and controller-integration challenges, would provide additional insight into practical deployment in shipboard microgrids. Owing to the lightweight ANN architecture and low computational complexity of the proposed scheduling framework, the developed DREMS offers potential suitability for implementation on embedded shipboard energy-management controllers. This approach can also be extended to isolated microgrid systems.

Conflict of Interest

The authors declare that there is no conflict of interest regarding publication of this article.

Author Contributions

Naveen Kumar Thotakanama contributed to conceptualization, methodology development, simulation studies, and manuscript writing.

Nagaraja Rao Sulake supervised the research work, provided technical guidance, and reviewed the manuscript.

Krishnan Manickavasagam contributed to validation, technical review, and manuscript editing. All authors have read and approved the manuscript.

Nomenclature

Symbol	Description
A	Swept area of wind turbine (m²)
b_1, b_2	ANN bias vectors
C_p	Wind turbine power coefficient
E_{rated}	Rated battery energy capacity (kWh)
i	Number of committed SPCS units
I_0	Diode saturation current (A)
I_{ph}	Photocurrent (A)
I_{pv}	PV module current (A)
j	Number of committed WPCS units
J	Mean squared error (MSE) loss function.
N	Number of training samples
N_{sp}	Maximum number of SPCS units
N_{wp}	Maximum number of WPCS units
$\hat{P}(k)$	ANN estimated power output
P_{aero}	Aerodynamic wind power (kW)
P_{ch}	Battery charging power (kW)
$P_{ch,max}$	Maximum battery charging power (kW)
P_{crit}	Critical load demand (kW)
P_{dis}	Battery discharging power (kW)
$P_{dis,max}$	Maximum battery discharging power (kW)
$P_{flex,adj}$	Adjusted flexible load demand (kW)
P_{pv}	PV output power (kW)
P_{ren}	Total renewable power (kW)
P_{req}	Effective load demand after DR adjustment (kW)
P_{sp}	Power output of one SPCS unit (kW)
P_w	Wind electrical power output (kW)
P_{wp}	Power output of one WPCS unit (kW)
R	Wind turbine blade radius (m)
R_s	PV series resistance (Ω)
SOC	Battery state of charge (%)
SOC_{max}	Maximum allowable state of charge
SOC_{min}	Minimum allowable state of charge
t	Time
$u(k)$	Normalized ANN input
V_{pv}	PV module voltage (V)
V_t	Thermal voltage (V)
v	Wind speed (m/s)
W_1, W_2	ANN weight matrices
ΔP	Power mismatch between demand and generation
η_{ch}	Battery charging efficiency
η_{dis}	Battery discharging efficiency
η^g	Generator–rectifier efficiency
λ	Tip-speed ratio
ρ	Air density (kg/m³)
$\phi(\cdot)$	Hidden-layer activation function
ω_r	Rotor angular speed (rad/s)

References

[1] A. M. Aboelezz, B. E. Sedhom, M. M. El-Saadawi, A. A. Eladl, and P. Siano, "State-of-the-art review on shipboard microgrids: Architecture, control, management, protection, and future perspectives," *Smart Cities*, vol. 6, no. 3, pp. 1435–1484, Jun. 2023. doi: https://doi.org/10.3390/smartcities6030069.

[2] H. Yin, H. Lan, Y.-Y. Hong, Z. Wang, P. Cheng, D. Li, and D. Guo, "A comprehensive review of shipboard power systems with new energy sources," *Energies*, vol. 16, no. 5, no. 2307, Mar. 2023. doi: https://doi.org/10.3390/en16052307.

[3] Y. Terriche *et al*., "Design of cost-effective compensators to enhance voltage stability and harmonics contamination of high-power more electric marine vessels," *IEEE Transactions on Industry Applications*, vol. 57, no. 4, pp. 4130–4142, Jul./Aug. 2021. doi: https://doi.org/10.1109/TIA.2021.3081079.

[4] H.-K. Ku, C.-H. Park, and J.-M. Kim, "Full simulation modeling of all-electric ship with medium voltage DC power system," *Energies*, vol. 15, no. 12, no. 4184, Jun. 2022. doi: https://doi.org/10.3390/en15124184.

[5] A. Haseltalab, M. A. Botto, and R. R. Negenborn, "Model predictive DC voltage control for all-electric ships," *Control Engineering Practice*, vol. 90, pp. 133–147, Sep. 2019. doi: https://doi.org/10.1016/j.conengprac.2019.06.018.

[6] Y. L. Karnavas and E. Nivolianiti, "Optimal load frequency control of a hybrid electric shipboard microgrid using jellyfish search optimization algorithm," *Applied Sciences*, vol. 13, no. 10, no. 6128, May 2023. doi: https://doi.org/10.3390/app13106128.

[7] L. Kistner, A. Bensmann, and R. Hanke-Rauschenbach, "Potentials and limitations of battery-electric container ship propulsion systems," *Energy Conversion and Management: X*, vol. 21, no. 100507, Jan. 2024. doi: https://doi.org/10.1016/j.ecmx.2023.100507.

[8] K. Manickavasagam, N. K. Thotakanama, and V. Puttaraj, "Intelligent energy management system for renewable energy driven ship," *IET Electrical Systems in Transportation*, vol. 9, no. 1, pp. 24–34, Mar. 2019. doi: https://doi.org/10.1049/iet-est.2018.5022.

[9] A. Cabrera-Tobar, A. Massi Pavan, G. Petrone, and G. Spagnuolo, "A review of the optimization and control techniques in the presence of uncertainties for the energy management of microgrids," *Energies*, vol. 15, no. 23, no. 9114, Dec. 2022. doi: https://doi.org/10.3390/en15239114.

[10] Y. Wu, J. Cui, and C. Liu, "State-of-the-art review on energy management systems, challenges and top trends of renewable energy-based microgrids," *EAI Endorsed Transactions on Energy Web*, vol. 10, no. 1, 2024. doi: https://doi.org/10.4108/ew.4124.

[11] N. Khosravi, A. Oubelaid, and Y. Belkhier, "Energy management in networked microgrids: A comparative study of hierarchical deep learning and predictive analytics techniques," *Energy Conversion and Management: X*, vol. 25, no. 100828, Jan. 2025. doi: https://doi.org/10.1016/j.ecmx.2024.100828.

[12] O. M. Neda, J. Adabi, H. Gholinezhadomran, and M. Marzband, "Machine learning-enhanced coordination of home-microgrids for resource compensation in large-scale energy systems," *Sustainable Cities and Society*, vol. 134, no. 106744, Nov. 2025. doi: https://doi.org/10.1016/j.scs.2025.106744.

[13] O. M. Neda, J. Adabi, M. Marzband, and H. Gholinezhadomran, "Hierarchical energy management system for coordinated operation of multiple grid-tied home microgrids," *Renewable Energy Focus*, vol. 56, no. 100766, Mar. 2026. doi: https://doi.org/10.1016/j.ref.2025.100766.

[14] I. Toure, A. Payman, M.-B. Camara, and B. Dakyo, "Energy management in a renewable-based microgrid using a model predictive control method for electrical energy storage devices," *Electronics*, vol. 13, no. 23, no. 4651, Nov. 2024. doi: https://doi.org/10.3390/electronics13234651.

[15] T. A. Nakabi and P. Toivanen, "Deep reinforcement learning for energy management in a microgrid with flexible demand," *Sustainable Energy, Grids and Networks*, vol. 25, no. 100413, Mar. 2021. doi: https://doi.org/10.1016/j.segan.2020.100413.

[16] B. Dey, S. Misra, and F. P. Garcia Marquez, "Microgrid system energy management with demand response program for clean and economical operation," *Applied Energy*, vol. 334, no. 120717, Mar. 2023. doi: https://doi.org/10.1016/j.apenergy.2023.120717.

[17] K. M. R. Pothireddy and S. Vuddanti, "Alternating direction method of multipliers based distributed energy scheduling of grid-connected microgrid by considering the demand response," *Discover Applied Sciences*, vol. 6, no. 343, Jun. 2024. doi: https://doi.org/10.1007/s42452-024-05975-2.

[18] E. Garcia, A. Águila, L. Ortiz, and D. Carrión, "Optimal resource assignment in hybrid microgrids based on demand response proposals," *Sustainability*, vol. 16, no. 5, Art. no. 1797, Mar. 2024. doi: https://doi.org/10.3390/su16051797.

[19] A. Aghazadeh Ardebili, M. Zappatore, A. I. H. A. Ramadan, A. Longo, and A. Ficarella, "Digital twins of smart energy systems: A systematic literature review on enablers, design, management and computational challenges," *Energy Informatics*, vol. 7, no. 94, Oct. 2024. doi: https://doi.org/10.1186/s42162-024-00385-5.

[20] O. Das, M. H. Zafar, F. Sanfilippo, S. Rudra, and M. L. Kolhe, "Advancements in digital twin technology and machine learning for energy systems: A comprehensive review of applications in smart grids, renewable energy, and electric vehicle optimization," *Energy Conversion and Management: X*, vol. 24, no. 100715, Oct. 2024. doi: https://doi.org/10.1016/j.ecmx.2024.100715.

[21] C. N. Ugwu, F. C. Ogenyi, J. N. Ugwu, P.-C. O. Ugwu, and M. B. Okon, "Integration of AI-driven digital twins for real-time optimization of renewable energy grids," *Frontiers in Energy Research*, vol. 14, Art. no. 1748233, Feb. 2026. doi: https://doi.org/10.3389/fenrg.2026.1748233.

[22] S. Das and S. Gupta, "Adaptive Protection Scheme Using Optimal Coordination of Directional Overcurrent Relays in Grid-Connected Mode by Applying Micro-Genetic Algorithm," *2025 Fourth International Conference on Power, Control and Computing Technologies (ICPC2T)*, Raipur, India, 2025, pp. 1-6, doi: 10.1109/ICPC2T63847.2025.10958655. doi: https://doi.org/10.1109/ICPC2T63847.2025.10958655

[23] H. Jiang *et al*., "Digital twin of microgrid for predictive power control to buildings," *Sustainability*, vol. 16, no. 2, Art. no. 482, Jan. 2024. doi: https://doi.org/10.3390/su16020482.

[24] R. Hashmi, H. Liu, and A. Yavari, "Digital twins for enhancing efficiency and assuring safety in renewable energy systems: A systematic literature review," *Energies*, vol. 17, no. 11, Art. no. 2456, May 2024. doi: https://doi.org/10.3390/en17112456.

[25] N. Kumari, A. Sharma, B. Tran, N. Chilamkurti, and D. Alahakoon, "A comprehensive review of digital twin technology for grid-connected microgrid systems: State of the art, potential and challenges faced," *Energies*, vol. 16, no. 14, Art. no. 5525, Jul. 2023. doi: https://doi.org/10.3390/en16145525.

[26] S. Aslam, P. P. Aung, A. S. Rafsanjani, and A. P. P. Abdul Majeed, "Machine learning applications in energy systems: Current trends, challenges, and research directions," *Energy Informatics*, vol. 8, Art. no. 62, May 2025. doi: https://doi.org/10.1186/s42162-025-00524-6.

[27] M. Hadi *et al*., "Artificial intelligence for microgrids design, control, and maintenance: A comprehensive review and prospects," *Energy Conversion and Management: X*, vol. 27, Art. no. 101056, Jul. 2025. doi: https://doi.org/10.1016/j.ecmx.2025.101056.

[28] R. Elazab, A. A. Dahab, M. A. Adma, and H. A. Hassan, "Enhancing microgrid energy management through solar power uncertainty mitigation using supervised machine learning," *Energy Informatics*, vol. 7, Art. no. 99, Oct. 2024. doi: https://doi.org/10.1186/s42162-024-00333-3.

[29] A. I. A. Anil, M. R. Al Muttaki, S. Afrin, and S. Hasan, "The next generation of energy storage for smart and sustainable power grids: A systematic review," *Energy Conversion and Management: X*, vol. 30, no. 101771, May 2026, doi: https://doi.org/10.1016/j.ecmx.2026.101771

[30] F. Moazzen and M. J. Hossain, "Multivariate deep learning long short-term memory-based forecasting for microgrid energy management systems," *Energies*, vol. 17, no. 17, Art. no. 4360, Aug. 2024. doi: https://doi.org/10.3390/en17174360.

[31] A. R. Singh, R. S. Kumar, M. Bajaj, C. B. Khadse, and I. Zaitsev, "Machine learning-based energy management and power forecasting in grid-connected microgrids with multiple distributed energy sources," *Scientific Reports*, vol. 14, Art. no. 19207, 2024. doi: https://doi.org/10.1038/s41598-024-70336-3.

[32] L. A. Aloo, P. K. Kihato, S. I. Kamau, and R. S. Orenge, "Modeling and control of a photovoltaic-wind hybrid microgrid system using GA-ANFIS," *Heliyon*, vol. 9, no. 4, Art. no. e14678, Apr. 2023. doi: https://doi.org/10.1016/j.heliyon.2023.e14678.

[33] L. B. K. Fisch and M. L. Heldwein, "10-MW direct-drive PMSG-based wind energy conversion system model," in *Proc. 2020 IEEE 21st Workshop on Control and Modeling for Power Electronics (COMPEL)*, Aalborg, Denmark, pp. 1–8. Nov. 2020, doi: https://doi.org/10.1109/COMPEL49091.2020.9265784.

[34] A. G. Sanchez, M. G. Molina, and A. M. Rizzato Lede, "Dynamic model of wind energy conversion systems with PMSG-based variable-speed wind turbines for power system studies," *International Journal of Hydrogen Energy*, vol. 37, no. 13, pp. 10064–10069, Jul. 2012. doi: https://doi.org/10.1016/j.ijhydene.2011.12.077.

[35] N. Hashmi and S. A. Khan, "Power energy management for a grid-connected PV system using rule-base fuzzy logic," in *Proceedings - AIMS 2015, 3rd International Conference on Artificial Intelligence, Modelling and Simulation*, Institute of Electrical and Electronics Engineers Inc., Kota Kinabalu, Malaysia, pp. 31–36, Oct. 2016, doi: https://doi.org/10.1109/AIMS.2015.15